

SEMI-SUPERVISED CERVICAL SEGMENTATION ON ULTRASOUND BY A DUAL FRAMEWORK FOR NEURAL NETWORKS

Fangyijie Wang^{*†} Kathleen M. Curran^{*†} Guénolé Silvestre^{*§}

^{*} Taighde Éireann – Research Ireland Centre for Research Training in Machine Learning

[§] School of Computer Science, University College Dublin, Dublin, Ireland

[†] School of Medicine, University College Dublin, Dublin, Ireland

ABSTRACT

Accurate segmentation of ultrasound (US) images of the cervical muscles is crucial for precision healthcare. The demand for automatic computer-assisted methods is high. However, the scarcity of labeled data hinders the development of these methods. Advanced semi-supervised learning approaches have displayed promise in overcoming this challenge by utilizing labeled and unlabeled data. This study introduces a novel semi-supervised learning (SSL) framework that integrates dual neural networks. This SSL framework utilizes both networks to generate pseudo-labels and cross-supervise each other at the pixel level. Additionally, a self-supervised contrastive learning strategy is introduced, which employs a pair of deep representations to enhance feature learning capabilities, particularly on unlabeled data. Our framework demonstrates competitive performance in cervical segmentation tasks. Our codes are publicly available on https://github.com/13204942/SSL_Cervical_Segmentation.

Index Terms— Semi-supervised Learning, Ultrasound Image, Cervical Segmentation, Contrastive Learning.

1. INTRODUCTION

Transvaginal ultrasound is the preferred method for visualizing the cervix in most patients as it provides detailed insight into cervical anatomy and structure [1]. Accurate segmentation of ultrasound (US) images of the cervical muscles is crucial for analyzing the deep muscle structures, evaluating their function, and monitoring customized treatment protocols for individual patients [2].

The manual annotation of cervical structures in transvaginal ultrasound images is a labor-intensive and time-consuming process, which restricts the availability of extensive labeled datasets essential for building robust machine learning models. To address this challenge, semi-supervised learning (SSL) techniques have shown potential by incorporating labeled and unlabeled data, thus enhancing the extraction of valuable insights from unannotated data [3, 4].

This study presents an SSL framework for cervical segmentation on ultrasound images. First, the SSL framework is

designed for network training on many unlabeled data. Then, pixel-level cross-supervised learning is introduced within the framework. Therefore, the network is trained with the help of the other network via pseudo-labeling. A contrastive learning strategy is introduced within this framework, incorporating a pair of embedded features to maximize the feature learning capabilities using both labeled and unlabeled data. Moreover, the framework is validated using a dataset in a public challenge, demonstrating competitive performance.

2. METHODOLOGY

The SSL framework of dual neural networks is illustrated in Fig.1, where $(\mathbf{X}_L, \mathbf{Y}_{gt}) \in \mathbf{L}$ denotes the labeled training dataset, while $(\mathbf{X}_{UL}) \in \mathbf{U}$ denotes the unlabeled training dataset. $\mathbf{X}_L, \mathbf{X}_{UL} \in \mathbb{R}^{3 \times n_h \times n_w}$ represents a 2D ultrasound image of size $n_h \times n_w$ with 3 channels. The dual neural networks are denoted by $f_\theta^1(\cdot)$ and $f_\phi^2(\cdot)$, respectively. $\mathbf{Y}_{pseudo}, \mathbf{Y}_{gt} \in \mathbb{R}^{3 \times n_h \times n_w}$ represents a three-class labeled segmentation masks with pixel values ranging from 0 to 2. The segmentation masks predicted by the segmentation networks $f_\theta^1(\cdot)$ and $f_\phi^2(\cdot)$ are $f_\theta^1(\mathbf{X})$ and $f_\phi^2(\mathbf{X})$, respectively, with θ and ϕ as their parameters. In our proposed method, the prediction of a network is considered as a pseudo label to expand the unlabeled dataset to $(\mathbf{X}_U, \mathbf{Y}_{pseudo})$ to train the other network. We utilize each network to extract the deep representation features of \mathbf{X}_L and \mathbf{X}_{UL} for contrastive learning. To select and save the best network from $f_\theta^1(\cdot)$ and $f_\phi^2(\cdot)$, we evaluate their segmentation performance by measuring the difference between $(f_\theta^1(\mathbf{X}), \mathbf{Y}_{gt})$ and $(f_\phi^2(\mathbf{X}), \mathbf{Y}_{gt})$ in our validation set.

Our training objective is minimizing the total loss \mathcal{L}_{total} by updating the network parameters θ and ϕ . The total loss \mathcal{L}_{total} consist of the supervision loss \mathcal{L}_{sup} , semi-supervised loss \mathcal{L}_{semi} , and self-supervised contrastive loss \mathcal{L}_{contra} . Mathematically, it can be expressed as:

$$\mathcal{L}_{total} = (\mathcal{L}_{sup}^1 + \mathcal{L}_{sup}^2) + \lambda(\mathcal{L}_{semi}^1 + \mathcal{L}_{semi}^2) + \mathcal{L}_{contra} \quad (1)$$

where λ represents the weighting factor for a ramp-up function used exclusively for the unlabeled training set [5]. This

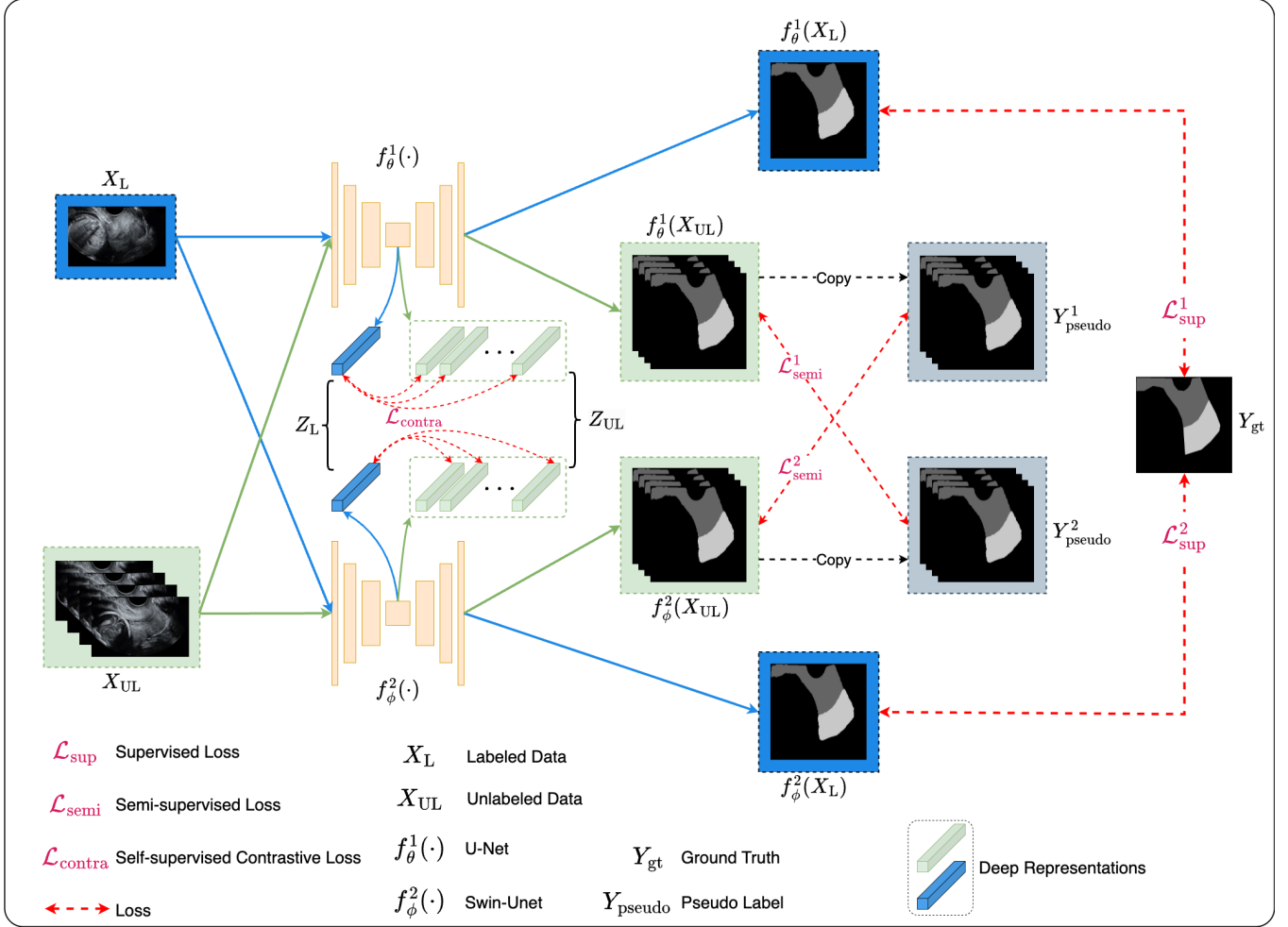


Fig. 1. Framework for deep representations contrastive cross-supervised neural networks for semi-supervised ultrasound image segmentation.

function facilitates the gradual transition of $f_{\theta}^1(\cdot)$ and $f_{\phi}^2(\cdot)$ from being initialized with the labeled training set to prioritizing learning from the unlabeled training set. In Fig.1, all loss functions are highlighted by a red dashed line. $\mathcal{L}_{\text{sup}}^1$ and $\mathcal{L}_{\text{sup}}^2$ are the supervision losses for $f_{\theta}^1(\cdot)$ and $f_{\phi}^2(\cdot)$ based on the labeled training set. \mathcal{L}_{sup} is designed with a combination of the Dice Similarity Coefficient (DSC) and cross-entropy (CE) losses, as follows:

$$\begin{aligned} \mathcal{L}_{\text{sup}}^1 &= \text{CE}(f_{\theta}^1(\mathbf{X}_L), \mathbf{Y}_{\text{gt}}) + \text{DSC}(f_{\theta}^1(\mathbf{X}_L), \mathbf{Y}_{\text{gt}}) \\ \mathcal{L}_{\text{sup}}^2 &= \text{CE}(f_{\phi}^2(\mathbf{X}_L), \mathbf{Y}_{\text{gt}}) + \text{DSC}(f_{\phi}^2(\mathbf{X}_L), \mathbf{Y}_{\text{gt}}) \end{aligned} \quad (2)$$

2.1. CNN and Transformer Segmentation Network

The UNet [6] presents a groundbreaking modification of the traditional encoder-decoder segmentation network, incorporating diverse network blocks tailored for medical image analysis. We adopt UNet as the convolutional neural network

(CNN) $f_{\theta}^1(\cdot)$ within our framework. In recent years, several variants of UNet have demonstrated superior segmentation performance in medical imaging analysis [7]. We leverage a Swin-UNet architecture [8] as $f_{\phi}^2(\cdot)$ to implement our SSL strategy. The detailed architecture of Swin-UNet is elucidated in the study by Cao et al. [8]. We initialize both networks with random weights.

2.2. Cross-Supervised Learning

Inspired by consistency regularization and multi-view learning principles, including cross-pseudo-supervision [9, 10], this study applies these concepts to construct dual architectures that facilitate mutual learning. CNNs excel in learning spatial hierarchies of features, while Transformer-based networks excel in capturing broad, non-local interactions. Hence, we propose a simple yet powerful cross-supervised learning approach that combines CNNs and Transformers to assist each other mutually. The semi-supervised loss function,

denoted as $\mathcal{L}_{\text{semi}}$, can be expressed as:

$$\begin{aligned}\mathcal{L}_{\text{semi}}^1 &= \text{CE}(f_{\theta}^1(\mathbf{X}_{\text{UL}}), \mathbf{Y}_{\text{pseudo}}^2) + \text{DSC}(f_{\theta}^1(\mathbf{X}_{\text{UL}}), \mathbf{Y}_{\text{pseudo}}^2) \\ \mathcal{L}_{\text{semi}}^2 &= \text{CE}(f_{\phi}^2(\mathbf{X}_{\text{UL}}), \mathbf{Y}_{\text{pseudo}}^1) + \text{DSC}(f_{\phi}^2(\mathbf{X}_{\text{UL}}), \mathbf{Y}_{\text{pseudo}}^1)\end{aligned}\quad (3)$$

We also investigated the approach of cross-teaching between two networks, including identical two CNNs or Transformer networks. Nevertheless, our proposed method, which integrates CNN and Transformer-based models, surpasses the effectiveness of this approach.

2.3. Contrastive Learning

Contrastive learning is widely acknowledged as a powerful paradigm for extracting robust and discriminative features, marking a significant advancement in the field of self-supervised learning [11]. The fundamental concept of contrastive learning is that both positive and negative samples are discriminative. The utilization of contrastive learning in the field of medical image analysis enhances the capability of feature extraction, ultimately leading to improved model performance [12, 13, 10].

In the paper [14], contrastive learning can be considered as a task to search a dictionary. Given an encoded query q , a set of encoded keys $\{k_1, k_2, \dots\}$ is retrieved from the memory bank. Among these keys, a specific positive key k^+ aligns with the query q , while the remaining negative keys k^- represent different images. A contrastive loss function InfoNCE [11] is utilized to bring q closer to positive key k^+ and simultaneously distance it from the negative keys k^- :

$$\mathcal{L}_q^{\text{NCE}} = -\log \frac{\exp(q \cdot k^+ / \tau)}{\exp(q \cdot k^+ / \tau) + \sum_{k^-} \exp(q \cdot k^- / \tau)} \quad (4)$$

where τ denotes a temperature hyper-parameter. In our SSL framework, we refer to the original InfoNCE loss, which is formalized as follows:

$$\mathcal{L}_{\text{contra}} = \sum_i^L \sum_j^{\text{UL}} \text{InfoNCE}(Z_L^i, Z_{\text{UL}}^j) \quad (5)$$

where InfoNCE represents the original InfoNCE loss function, Z_L^i and Z_{UL}^j represent deep representations obtained by models $f_{\theta}^1(\cdot)$ and $f_{\phi}^2(\cdot)$ for \mathbf{X}_L and \mathbf{X}_{UL} , respectively. Incorporating the InfoNCE loss aids in generating complex pixel representations by leveraging ample unlabeled data, thereby enhancing the resilience and label efficiency of segmentation models.

3. EXPERIMENTS AND RESULTS

3.1. Datasets

The FUGC dataset: We utilize one transvaginal dataset in this study. It contains images that include anatomical

structures of the cervix, namely the anterior and posterior lips. They are captured using a curved transducer with a frequency range of 2 to 10 MHz, specifically a vaginal probe utilized for cervical ultrasound screening in second-trimester patients. Operators are directed to refrain from applying post-processing techniques or introducing artifacts like smoothing, noise, pointers, or calipers whenever feasible. Other image settings, such as gain, frequency, and gain compensation, are adjusted according to individual discretion. The training set comprises 500 images, the external validation set comprises 90 images, and the testing set comprises 300 images. Among these 500 images, only 50 images are annotated by experienced operators. The resolutions for all images are 336×544 . During model training, 500 images are resized to the size of 224×224 . We use the 50 labeled images to evaluate the segmentation performance of the dual neural networks and save the best model among them.

Data Augmentation: In this study, data augmentations are implemented on the labeled dataset. These augmentation techniques include rotation within range $(-20^\circ, 20^\circ)$, random brightness contrast, random blur with probability $\mathcal{P}(\cdot) = 0.3$, and gaussian noise with probability $\mathcal{P}(\cdot) = 0.3$.

3.2. Implementation Details

All experiments were implemented in Pytorch and trained on a single RTX 3090 24G GPU. We use a batch size of 8 for training, including two labeled samples and six unlabeled data samples. We adopted a stochastic gradient descent optimizer with a learning rate 0.001, momentum of 0.9, and weight decay of 0.0001. Besides, we set a maximum of 30,000 iterations for training. All neural networks are initialized with random parameters. The experiments used the same hyperparameter for a fair comparison. We also investigated various hyperparameter settings, including a labeled batch size of 1, an unlabeled batch size of 9, and an initial learning rate of 0.01. However, it was our adopted hyperparameter setting that ultimately delivered optimal performance, characterized by fast convergence.

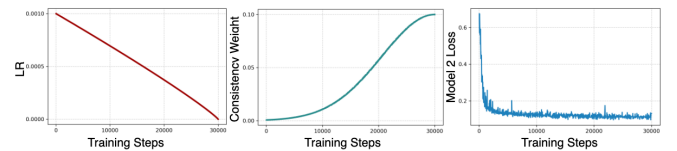


Fig. 2. Plots of the hyperparameter settings. From left to right: (a) Learning rate. (b) Consistency weight λ in Equation 1. (c) Training loss of model $f_{\phi}^2(\cdot)$.

3.3. Evaluation Metrics

To measure the performance of our framework, we employ the area metric and the boundary metric: DSC and Haus-

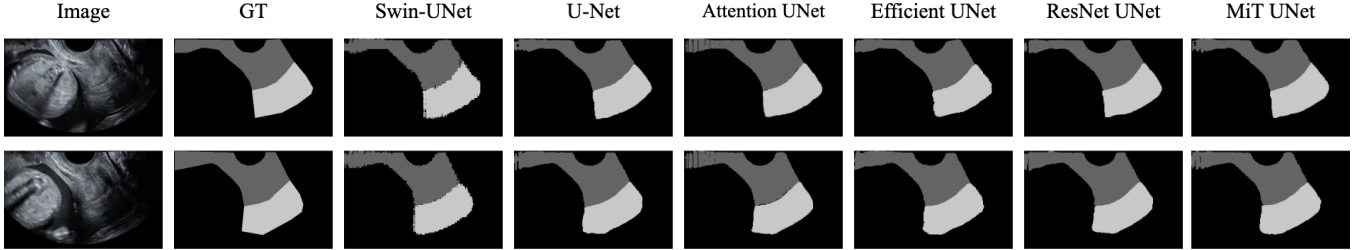


Fig. 3. Example ultrasound images from our validation set, ground truth (GT), and corresponding segmentation results of Swin-UNet, U-Net, Attention UNet, Efficient UNet, ResNet UNet, and MiT UNet.

dorff Distance (HD). The DSC measures the percentage of area overlap between the predicted and ground truth segmentation maps. HD measures the error between the predicted and ground truth segmentation boundaries in pixels. Additionally, we incorporate the execution time to measure the inference speed.

Table 1. Segmentation performance of different neural networks on the external validation set.

$f_{\theta}^1(\cdot)$	$f_{\phi}^2(\cdot)$	DSC \uparrow	HD \downarrow	Time \downarrow
U-Net	U-Net	0.76	63.99	5.65
U-Net	Attention U-Net	0.78	78.68	8.89
U-Net	Efficient-Unet	0.84	60.52	74.62
U-Net	ResNet-Unet	0.82	69.94	7.79
U-Net	MiT-Unet	0.82	62.88	7.04
U-Net	Swin-UNet	0.86	46.44	16.95

3.4. Validation

Fig. 2 illustrates our optimized hyperparameter configuration. The learning rate decays to facilitate the convergence of models $f_{\theta}^1(\cdot)$ and $f_{\phi}^2(\cdot)$ at the completion of training. The consistency weight λ guides the models towards learning effectively from the unlabeled training set. The training loss is minimized without additional decays over the course of our maximum epochs.

Table 1 illustrates the quantitative results of our SSL framework with several types of UNet, including U-Net [6], Attention U-Net [15], Efficient-Unet [16], ResNet-Unet [17], MiT-Unet [18] and Swin-UNet [8] when 50 cases in the training set are labeled data for training. The Swin-UNet outperforms other UNet variants, achieving a DSC of 0.86 and an HD of 46.44. Although the Swin-UNet has a longer inference time than U-Net and Attention U-Net, the value of 16.95 remains within an acceptable range. We computed the average evaluation metrics for models on the validation set to determine the optimal model for future testing. Then we choose the best one for the challenge competition.

In Fig. 3, we visualize two randomly selected example ultrasound images from our validation set (50 images). The Swin-UNet model demonstrates highly accurate predictions that closely align with the ground truth.

Table 2. Performance comparison between the baseline method and our proposed framework on the testing dataset. Baseline: A model provided by the challenge organizer.

Rank	Method	DSC \uparrow	HD \downarrow	Time \downarrow
1	N/A	0.90	44.94	365.91
2	N/A	0.90	40.20	340.24
3	N/A	0.87	45.70	518.38
11	Ours	0.78	66.74	43.51
14	Baseline	0.72	115.41	402.30

3.5. Comparison with Other Methods

In Table 2, we compare our method to the top 3 methods and the baseline method on the testing dataset provided by the challenge organizer. Compared to the baseline method, our SSL framework increases the DSC by 0.06 while reducing the inference time by 82%. Moreover, the HD significantly decreased from 115.41 to 66.74.

4. CONCLUSION

We conducted a study to explore the implementation of UNet-based architectures within a semi-supervised approach for cervical segmenting on ultrasound images. We introduced an innovative learning strategy that integrates cross-supervision and contrastive learning techniques to optimize the performance of SSL. Through our experimental analyses, we highlighted the efficacy of our SSL framework. In future studies, we aim to enhance our research by refining our methodologies in restricted supervised learning scenarios while persisting in utilizing the distinctive features offered by UNet variants.

5. ACKNOWLEDGMENT

This publication has emanated from research conducted with the financial support of Taighde Éireann – Research Ireland under Grant number 18/CRT/6183. For the purpose of Open Access, the author has applied a CC BY public copyright licence to any Author Accepted Manuscript version arising from this submission

6. REFERENCES

- [1] Juan Luis Alcázar, Sara Arribas, José Angel Mínguez, and Matías Jurado, “The role of ultrasound in the assessment of uterine cervical cancer,” *The Journal of Obstetrics and Gynecology of India*, vol. 64, no. 5, pp. 311–316, Oct. 2014.
- [2] Eva Boneš, Marco Gergolet, Ciril Bohak, Žiga Lesar, and Matija Marolt, “Automatic segmentation and alignment of uterine shapes from 3D ultrasound data,” *Computers in Biology and Medicine*, vol. 178, pp. 108794, Aug. 2024.
- [3] Jesper E van Engelen and Holger H Hoos, “A survey on semi-supervised learning,” *Machine Learning*, vol. 109, no. 2, pp. 373–440, Feb. 2020.
- [4] Xiangli Yang, Zixing Song, Irwin King, and Zenglin Xu, “A survey on deep semi-supervised learning,” *IEEE Transactions on Knowledge and Data Engineering*, vol. 35, no. 9, pp. 8934–8954, 2023.
- [5] Samuli Laine and Timo Aila, “Temporal ensembling for semi-supervised learning,” in *International Conference on Learning Representations (ICLR)*, 2017.
- [6] Olaf Ronneberger, Philipp Fischer, and Thomas Brox, “U-Net: Convolutional networks for biomedical image segmentation,” in *LNCS: Medical Image Computing and Computer-Assisted Intervention (MICCAI)*. 2015, vol. 9351, pp. 234–241, Springer.
- [7] M. Krithika alias AnbuDevi and K. Suganthi, “Review of semantic segmentation of medical images using modified architectures of unet,” *Diagnostics*, vol. 12, no. 12, 2022.
- [8] Hu Cao, Yueyue Wang, Joy Chen, Dongsheng Jiang, Xiaopeng Zhang, Qi Tian, and Manning Wang, “Swin-Unet: Unet-Like pure transformer for medical image segmentation,” in *Computer Vision – ECCV 2022 Workshops*. 2023, pp. 205–218, Springer Nature Switzerland.
- [9] Xiaokang Chen, Yuhui Yuan, Gang Zeng, and Jingdong Wang, “Semi-supervised semantic segmentation with cross pseudo supervision,” in *Proceedings of the IEEE/CVF conference on computer vision and pattern recognition*, 2021, pp. 2613–2622.
- [10] Chao Ma and Ziyang Wang, “Semi-mamba-unet: Pixel-level contrastive and pixel-level cross-supervised visual mamba-based unet for semi-supervised medical image segmentation,” 2024.
- [11] Aaron van den Oord, Yazhe Li, and Oriol Vinyals, “Representation learning with contrastive predictive coding,” 2019.
- [12] Chenyu You, Yuan Zhou, Ruihan Zhao, Lawrence Staib, and James S. Duncan, “Simcvd: Simple contrastive voxel-wise representation distillation for semi-supervised medical image segmentation,” *IEEE Transactions on Medical Imaging*, vol. 41, no. 9, pp. 2228–2237, 2022.
- [13] Ziyang Wang and Congying Ma, “Dual-contrastive dual-consistency dual-transformer: A semi-supervised approach to medical image segmentation,” in *Proceedings of the IEEE/CVF international conference on computer vision*, 2023, pp. 870–879.
- [14] Kaiming He, Haoqi Fan, Yuxin Wu, Saining Xie, and Ross Girshick, “Momentum contrast for unsupervised visual representation learning,” in *Proceedings of the IEEE/CVF conference on computer vision and pattern recognition*, 2020, pp. 9729–9738.
- [15] Ozan Oktay, Jo Schlemper, Loic Le Folgoc, Matthew Lee, Mattias Heinrich, Kazunari Misawa, Kensaku Mori, Steven McDonagh, Nils Y Hammerla, Bernhard Kainz, Ben Glocker, and Daniel Rueckert, “Attention unet: Learning where to look for the pancreas,” in *Medical Imaging with Deep Learning*, 2018.
- [16] Mingxing Tan and Quoc Le, “Efficientnetv2: Smaller models and faster training,” in *Proceedings of the 38th International Conference on Machine Learning*, Marina Meila and Tong Zhang, Eds. 18–24 Jul 2021, vol. 139 of *Proceedings of Machine Learning Research*, pp. 10096–10106, PMLR.
- [17] Kaiming He, Xiangyu Zhang, Shaoqing Ren, and Jian Sun, “Deep residual learning for image recognition,” in *2016 IEEE Conference on Computer Vision and Pattern Recognition (CVPR)*, 2016, pp. 770–778.
- [18] Enze Xie, Wenhai Wang, Zhiding Yu, Anima Anandkumar, Jose M Alvarez, and Ping Luo, “Segformer: Simple and efficient design for semantic segmentation with transformers,” in *Neural Information Processing Systems (NeurIPS)*, 2021.